Nanoscopic studies of domain structure dynamics in ferroelectric La:HfO_2 capacitors

P. Buragohain, C. Richter, T. Schenk, H. Lu, T. Mikolajick, U. Schroeder, and A. Gruverman

Citation: Appl. Phys. Lett. **112**, 222901 (2018); doi: 10.1063/1.5030562
View online: https://doi.org/10.1063/1.5030562
View Table of Contents: http://aip.scitation.org/toc/apl/112/22
Published by the American Institute of Physics

Nanoscopic studies of domain structure dynamics in ferroelectric La:HfO_2 capacitors

P. Buragohain,[1] C. Richter,[2] T. Schenk,[2] H. Lu,[1] T. Mikolajick,[2,3] U. Schroeder,[2] and A. Gruverman[1,a)]
[1]*Department of Physics and Astronomy, University of Nebraska, Lincoln, Nebraska 68588, USA*
[2]*NaMLab gGmbH/TU Dresden, Noethnitzer Str. 64, 01187 Dresden, Germany*
[3]*Institute of Semiconductors and Microsystems, TU Dresden, 01062 Dresden, Germany*

(Received 22 March 2018; accepted 12 May 2018; published online 31 May 2018)

Visualization of domain structure evolution under an electrical bias has been carried out in ferroelectric La:HfO_2 capacitors by a combination of Piezoresponse Force Microscopy (PFM) and pulse switching techniques to study the nanoscopic mechanism of polarization reversal and the wake-up process. It has been directly shown that the main mechanism behind the transformation of the polarization hysteretic behavior and an increase in the remanent polarization value upon the alternating current cycling is electrically induced domain de-pinning. PFM imaging and local spectroscopy revealed asymmetric switching in the La:HfO_2 capacitors due to a significant imprint likely caused by the different boundary conditions at the top and bottom interfaces. Domain switching kinetics can be well-described by the nucleation limited switching model characterized by a broad distribution of the local switching times. It has been found that the domain velocity varies significantly throughout the switching process indicating strong interaction with structural defects. *Published by AIP Publishing.* https://doi.org/10.1063/1.5030562

The discovery of ferroelectricity (FE) in hafnium oxide (HfO_2) based thin films[1] opens a possibility of overcoming significant problems associated with application of perovskite ferroelectrics in electronic devices, such as poor CMOS compatibility, small bandgap, and low resistance to hydrogen.[2] Robust polarization and high switching endurance make them promising candidates for ferroelectric memory and logic devices.[3,4] This application potential has been emphasized by the development of functional HfO_2-based ferroelectric field effect transistors[5] and a recent demonstration of polarization-controlled tunneling electroresistance effect in ultrathin HfO_2-based tunnel junctions.[6,7] Realization of the full potential of the HfO_2-based films requires comprehensive studies of the mechanism of polarization reversal and the impact of microstructure on their switching properties. One of the characteristic features of these materials is the so-called "wake-up" effect[8–11] [also termed as alternating current (AC) training[12]], in which a polarization hysteresis loop, initially constricted, opens up upon AC field cycling exhibiting a significantly increased remanent polarization. Several groups have reported that the underlying cause for this effect might be a redistribution of mobile ions[13] and oxygen vacancies,[14–16] or a phase transition from a non-FE to a FE phase.[17,18] In spite of active studies by means of integral electrical methods, such as polarization hysteresis and transient current measurements,[19] there is dearth of information on the kinetics of domain nucleation and wall motion during polarization reversal in HfO_2-based films. Here, we use a combination of high-resolution domain imaging and local switching spectroscopy by Piezoresponse Force Microscopy (PFM) in conjunction with pulse switching measurements to get a nanoscopic insight into the mechanism of the wake-up phenomenon and switching behavior of La-doped HfO_2 (La:HfO_2) ferroelectric capacitors. We find that the AC field cycling leads to de-pinning of domains, resulting in an increase in the remanent polarization. It is also shown that polarization reversal behavior is consistent with the nucleation-limited switching model (NLS).[20]

Experiments have been carried out using $125 \times 110\ \mu m^2$ capacitors fabricated on Si substrates by atomic layer deposition (ALD).[21] A stack of 10-nm-thick La:HfO_2 film sandwiched between TiN electrodes has been annealed in N_2 atmosphere at 800 °C for 20 s. Subsequently, 10-nm-thick Ti and 25-nm-thick Pt layers were evaporated on TiN and patterned into top electrode pads.[21]

In these studies, a microscopic external probe has been used to apply the poling voltage pulses and the AC voltage to the top electrode during the PFM and pulse switching measurements [Fig. 1(a)], while the PFM cantilevers have been used to detect the local electromechanical response of the samples visualizing the domain structure and acquire the surface topography maps [Fig. 1(b)]. This approach allows alleviation of the problem associated with the quick deterioration of the tip-sample contact resistance as well as with the strong electrostatic effect on the measured PFM signal.[22] PFM imaging and local switching spectroscopy measurements have been carried out using a commercial atomic force microscope system (MFP-3D, Asylum Research) with single-crystalline diamond tips (D80, K-Tek Nanotechnology) and employing a 350 kHz AC voltage with the 0.5 V amplitude. Voltage pulses were applied using a Keysight 33621A arbitrary waveform generator, and the signals were recorded by a Tektronix TDS 3014B oscilloscope.

Conventional polarization-voltage (P-V) hysteresis loops have been obtained by integration of the transient current under application of a triangular voltage pulse. The pristine

a)Author to whom correspondence should be addressed: alexei_gruverman@unl.edu

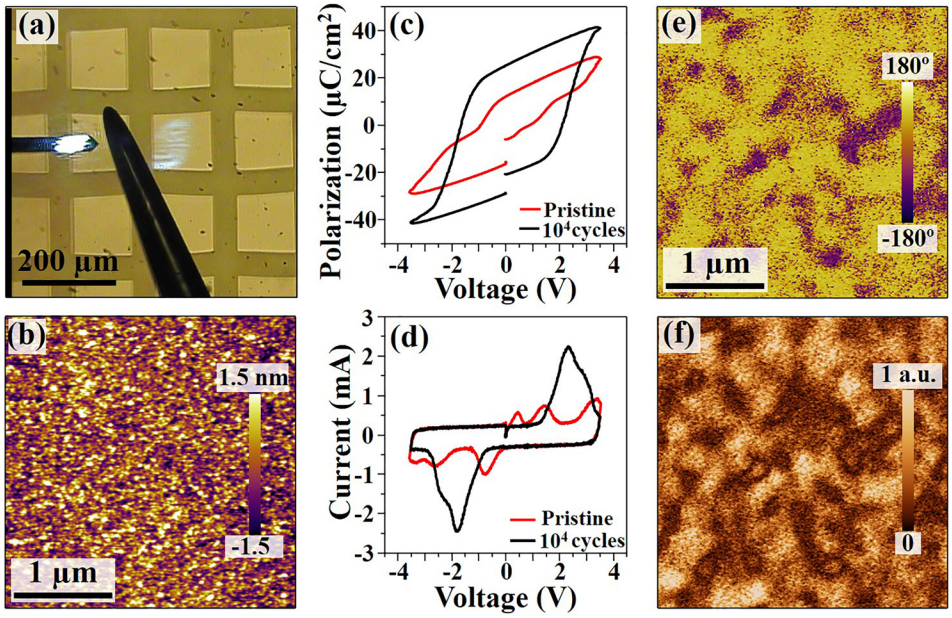

FIG. 1. (a) Optical microscopy photo of the $125 \times 110\ \mu m^2$ La:HfO_2 capacitors array showing the cantilever and an external microprobe on top of one of the capacitors. (b) Topographic image of the TiN top electrode using atomic force microscopy (AFM). (c) P-V hysteresis loops and (d) I-V loops acquired from the La:HfO_2 capacitor in the pristine state (red) and after 10^4 cycles of AC training (black). (e), (f) PFM phase (e) and amplitude (f) of a pristine capacitor.

state of the La:HfO_2 capacitors is characterized by a pinched hysteresis loop with a low value of remanent polarization [Fig. 1(c)], which is consistent with the earlier reported results.[10,13,14,21] Multiple switching peaks in the corresponding current-voltage (I-V) curve [Fig. 1(d)] can be attributed to a wide variability of the local pinning potential. PFM imaging of the pristine La:HfO_2 capacitors reveals a polydomain structure with an average domain size of several hundred nanometers [Figs. 1(e) and 1(f)] and no correlation with any topographic features. To induce the wake-up process, the capacitors were subjected to 10^4 cycles of AC training using rectangular voltage pulses of ± 3.5 V amplitude and 25 μs duration. As a result of this cyclic switching, the remanent polarization increased to about 25 $\mu C/cm^2$ while the transient current peaks merged into single switching peaks suggesting significant changes in the switching potential landscape.

To understand the underlying mechanism of the wake-up effect, the nanoscopic domain structure and its response to the applied electrical bias have been investigated by means of the PFM technique. Figures 2(a) and 2(b) show that the application of ± 3.0 V, 1 ms voltage pulses to the pristine capacitors results only in a minimal change in the domain configuration suggesting strong pinning of domains, which is consistent with the low remanent polarization value detected from the P-V loop measurements. The switchability of the capacitors dramatically changes after they were subjected to 10^4 cycles of AC training as is illustrated by the PFM images in Figs. 2(c) and 2(d). It can be seen that the domain structure changes completely in response to the application of the ± 3.0 V, 1 ms poling pulses, indicating increased switchability of domains as a result of the wake-up process. This result, in conjunction with X-ray diffraction results indicating a FE phase volume fraction of almost 90% in the studied films,[21] suggests that the increase in the remanent polarization upon AC cycling is mostly due to domain de-pinning, even though some contribution from the field-induced phase transformation cannot be ruled out.[18,21] Note, that the de-pinning process is not symmetric: some of the domains with the downward polarization were still pinned after AC cycling as they could not be switched upward by the application of a -3 V pulse [Fig. 2(c)], while switching to the downward direction by a 3 V pulse was complete [Fig. 2(d)]. It can be assumed that this asymmetry is a result of the asymmetric boundary conditions at the top and bottom interfaces due to the fabrication route. The bottom electrode is subject to oxidizing species during the ALD process, which is not the case for the top electrode, and a Ti-O(-N) layer has been shown to form under similar conditions also due to the thermal energy imposed by the crystallization anneal.[23–25] Another feature worth mentioning is strong spatial variability of the local switching parameters at the nanoscale level likely caused by structural imperfections associated with polycrystalline nature of the La:HfO_2 capacitors.

Analysis of the PFM images in Figs. 2(a) and 2(b) allows us to select different representative regions to illustrate this point. Shown in Figs. 2(e)–2(g) are the local PFM hysteresis loops for the pristine state (red curves) and after AC cycling (blue curves) for the three locations marked in Fig. 2(a). Location 1 exhibits symmetric coercive voltages and good switchability before and after the wake-up process [Fig. 2(e)], which is consistent with the switching behavior revealed by the PFM imaging in Figs. 2(a)–2(d). Location 2, however, shows strong negative imprint in the pristine state [Fig. 2(f)] consistent with the pinned downward polarization state. This imprint disappears after AC cycling suggesting domain de-pinning, which can be also seen in the PFM phase image [Fig. 2(d)]. In location 3, no evidence of the ferroelectric behavior can be observed even after the wake-up process [Fig. 2(g)], which could be a signature of a residual non-ferroelectric phase. Both findings, an initial local imprint that disappears during AC cycling and the existence of non-FE phase fractions are consistent with earlier reports based on first-order reversal curves[13] and Rietveld refinement.[21]

The switching spectroscopy PFM (SS-PFM) approach[26] provides further insight into the spatial variability of the local switching parameters. Two-dimensional maps of the local imprint bias have been generated by acquiring local hysteresis loops at each point while rastering the $500 \times 500\ nm^2$ region

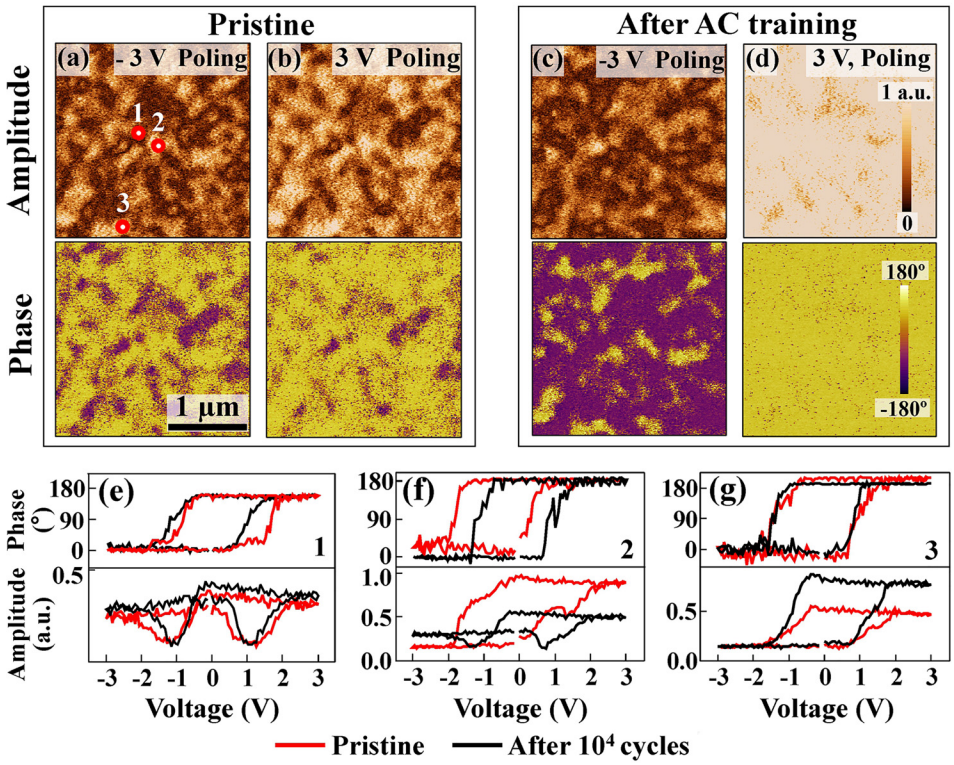

FIG. 2. (a)–(d) Comparison of capacitor switchability in the pristine state and after the wake-up process. PFM amplitude (top) and phase (bottom) images of a La:HfO_2 capacitor after application of a ±3V, 1 ms pulse in pristine state (a), (b) and after application of 10^4 cycles of AC training (c), (d). Bright (dark) color in the phase images corresponds to downward (upward) polarization. (e)–(g) Local PFM hysteresis loops acquired in location 1 (e), 2 (f), and 3 (g) marked with red dots in (a) for pristine (red) and after the wake-up process (black).

on the top electrode surface of the capacitors in the pristine state [Fig. 3(a)] and after the wake-up process [Fig. 3(b)]. Histogram analysis of the acquired maps reveals the reduction in the magnitude of imprint upon AC field cycling [Fig. 3(c)], even though about 90% of the imaged area still exhibits some negative imprint after the wake-up process. The SS-PFM maps and the corresponding histograms further corroborate the switching behavior seen in the PFM poling data (Fig. 2).

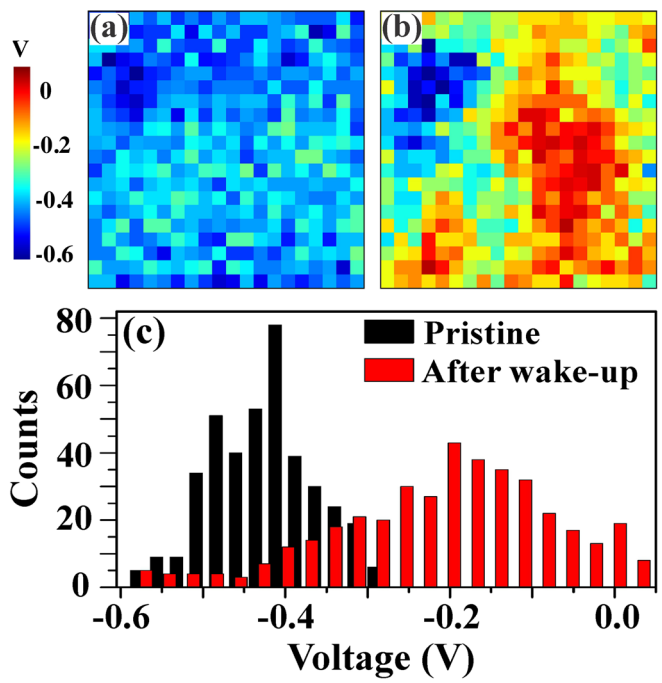

FIG. 3. (a), (b) $500 \times 500\,nm^2$ imprint maps obtained by PFM switching spectroscopy using a 20×20 grid for the pristine state (a) and after wake-up (b). (c) Comparison of histograms of the imprint maps in (a) and (b) illustrating a change in the overall imprint bias after the wake-up process.

The spatial variations of the imprint and coercive bias give a sense of the expected domain kinetics in the La:HfO_2 capacitors during polarization reversal, which has been investigated by means of the stroboscopic PFM approach.[27] In this approach, a sequence of input voltage pulses of incrementally increasing duration (each one shorter than the total switching time) is applied to a capacitor inducing partial polarization switching. PFM imaging of the resulting domain pattern representing a certain stage of polarization reversal is performed after each pulse. Figure 4(a) shows PFM images of instantaneous domain configurations developing in the previously AC-trained La:HfO_2 capacitors at different stages of polarization reversal process induced by 4 V switching pulses. It can be seen that switching occurs through the sidewise expansion of the residual (pinned) domains of the corresponding polarity that have not been removed during the wake-up process as well as via nucleation and growth of new domains. By analyzing the space-time dependence of the domain expansion in the PFM snapshots, we were able to estimate the lateral domain wall (DW) velocity. It was found that the DW velocity varied depending on the azimuthal direction and was not constant throughout the switching process suggesting a strong impact of structural defects, such as grain boundaries. This hypothesis is supported by the fact that the size of the growing domains reaches values of up to 300 nm, which is larger than the average grain size (~30–50 nm), implying that the DWs move across several grain boundaries before annihilation by domain coalescence. Figure 4(b) shows a representative plot of the variations in the DW velocity as a function of time. The maximum velocity measured is about 0.15 m/s, which is two orders of magnitude slower than the velocities observed in Pb(Zr,Ti)O_3 capacitors for the same ratio of the applied field to the coercive field.[27,28] This low DW velocity seems to be consistent

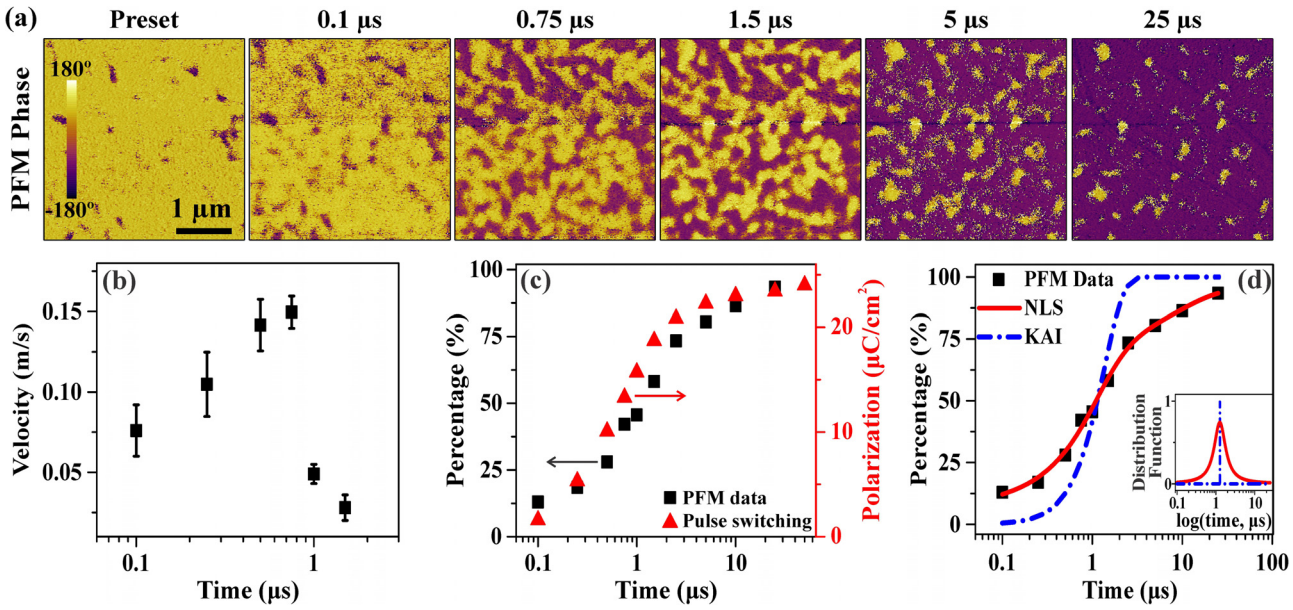

FIG. 4. (a) PFM phase images of instantaneous domain configurations developing at different stages of polarization reversal under application of 4.0 V pulses of increasing duration. (b) Time-dependent variations in domain wall velocity obtained by analyzing images in (a). (c) Comparison of experimental PFM data showing switched capacitor area as a function of time with the polarization obtained from pulse switching measurements. (d) Fitting of the PFM switching data by the KAI and NLS models. The inset shows the distribution functions for the corresponding models.

with recent reports on a small value of the Rayleigh constant measured in HfO_2-based films.[29] Further dielectric spectroscopy studies are necessary to clarify the mechanism of this significant speed discrepancy between HfO_2-based and $Pb(Zr,Ti)O_3$ films.

To quantify the domain switching kinetics, a time dependence of the switched capacitor volume fraction has been obtained by image analysis of the PFM data and plotting the obtained results as a function of the pulse duration. In addition, we performed pulse switching measurements using a four pulse waveform[20] to estimate the switched polarization as a function of the pulse duration to compare it with the PFM stroboscopic data. We found that the switched capacitor fraction with polarization along the direction of the applied field detected by PFM is proportional to the switched charge obtained by integration of current induced by pulse switching [Fig. 4(c)]. This allows us to treat the time-dependent PFM switching data, shown in Fig. 4(d), the same way as the switched polarization data and fit them with the well-known NLS model[20]

$$\Delta P(t) = 2Ps\int_{-\infty}^{\infty}\left[1-\exp\left\{-\left(\frac{t}{t_0}\right)^n\right\}\right]\cdot F(\log t_0)\cdot d(\log t_0), \tag{1}$$

where P_s is the spontaneous polarization, $F(log\ t_0)$ is a distribution function of the characteristic switching time, t_0, and n is the effective dimension of domain growth (n = 2 in this case). The term in the square brackets in Eq. (1) represents the Kolmogorov-Avrami-Ishibashi (KAI)[30–32] switching model, which does not consider spatial inhomogeneities in the film structure. To account for the polycrystalline nature of the La:HfO_2 films and non-uniform internal potential landscape manifested in the imprint map [Fig. 3(b)], a Lorentzian distribution of the local switching times[33] is used in the NLS fitting

$$F(\log t_0) = \frac{A}{\pi}\left[\frac{w}{(\log t_0 - \log t_1)^2 + w^2}\right], \tag{2}$$

where A is a normalization constant, w is the half-width at half-maximum, and $log\ t_1$ is the center of the distribution. When w approaches zero, $F(x)$ becomes a delta function and we obtain the KAI model. Figure 4(d) shows that the NLS model provides a better fit to the experimental data than the KAI model, in agreement with previous reports that involved only pulse switching measurements.[19,34]

In conclusion, a combination of PFM imaging and macroscopic polarization switching measurements provides direct evidence that the increase in the remanent polarization upon AC cycling in the La:HfO_2 capacitors is mainly a result of electrically induced domain de-pinning although some contribution from the field-induced phase transformation cannot be ruled out. PFM poling experiments and switching spectroscopy reveal a broad variation in the local switching parameters likely caused by the asymmetry in the boundary conditions at the capacitors top and bottom interfaces and by the polycrystalline nature of the La:HfO_2 films. The remanent (pinned) domains serve as the nucleation centers during polarization reversal and contribute to the switching behavior that is best described by the NLS model. The nanoscopic visualization of domain structure evolution during the wake-up process as well as during polarization reversal will allow optimization of the switching behavior of the La:HfO_2-based ferroelectric devices.

This work was supported by the National Science Foundation (NSF) through Materials Research Science and Engineering Center (MRSEC) under Grant No. DMR-1420645. T.S. gratefully acknowledges the German Research Foundation (Deutsche Forschungsgemeinschaft) for funding part of this research in the frame of the "Inferox" project (MI 1247/11-2).

[1]T. S. Boescke, J. Mueller, D. Braeuhaus, U. Schroeder, and U. Boetgger, Appl. Phys. Lett. **99**, 102903 (2011).
[2]M. H. Park, Y. H. Lee, H. J. Kim, Y. J. Kim, T. Moon, K. D. Kim, J. Müller, A. Kersch, U. Schroeder, T. Mikolajick, and C. S. Hwang, Adv. Mater. **27**, 1811 (2015).
[3]J. F. Scott, *Ferroelectric Memories* (Springer, Berlin, 2000).
[4]See http://www.itrs2.net/itrs-reports.html for "International Technology Roadmap for Semiconductors-2013 Emerging Research Devices."
[5]J. Müller, T. S. Böscke, S. Müller, E. Yurchuk, P. Polakowski, J. Paul, D. Martin, T. Schenk, K. Khullar, A. Kersch, W. Weinreich, S. Riedel, K. Seidel, A. Kumar, T. M. Arruda, S. V. Kalinin, T. Schlösser, R. Boschke, R. van Bentum, U. Schröder, and T. Mikolajick, in *IEEE International Electron Devices Meeting* (2013), p. 10.8.1.
[6]A. Chernikova, M. Kozodaev, A. Markeev, D. Negrov, M. Spiridonov, S. Zarubin, O. Bak, P. Buragohain, H. Lu, E. Suvorova, A. Gruverman, and A. Zenkevich, ACS Appl. Mater. Interfaces **8**, 7232 (2016).
[7]S. Fujii, Y. Kamimuta, T. Ino, Y. Nakasaki, R. Takaishi, and M. Saitoh, in *2016 IEEE Symposium on VLSI Technology*, Honolulu, USA, 14–16 June 2016 (IEEE, 2016), pp. 1–2.
[8]D. Zhou, J. Xu, Q. Li, Y. Guan, F. Cao, X. Dong, J. Müller, T. Schenk, and U. Schroeder, Appl. Phys. Lett. **103**, 192904 (2013).
[9]S. Müller, C. Adelmann, A. Singh, S. Van Elshocht, U. Schroeder, and T. Mikolajick, ECS J. Solid State Sci. Technol. **1**, N123 (2012).
[10]T. Schenk, U. Schroeder, M. Pešic, M. Popovici, Y. V. Pershin, and T. Mikolajick, ACS Appl. Mater. Interfaces **6**, 19744 (2014).
[11]M. H. Park, H. J. Kim, Y. J. Kim, Y. H. Lee, T. Moon, K. D. Kim, S. D. Hyun, F. Fengler, U. Schroeder, and C. S. Hwang, ACS Appl. Mater. Interfaces **8**, 15466 (2016).
[12]M. Kohli, P. Muralt, and N. Setter, Appl. Phys. Lett. **72**, 3217 (1998).
[13]T. Schenk, M. Hoffmann, J. Ocker, M. Pešic, T. Mikolajick, and U. Schroeder, ACS Appl. Mater. Interfaces **7**, 20224 (2015).
[14]S. Starschich, S. Menzel, and U. Böttger, Appl. Phys. Lett. **108**, 032903 (2016).
[15]M. Pešic, F. P. G. Fengler, L. Larcher, A. Padovani, T. Schenk, E. D. Grimley, X. Sang, J. M. LeBeau, S. Slesazeck, U. Schroeder, and T. Mikolajick, Adv. Funct. Mater. **26**, 4601 (2016).
[16]F. P. G. Fengler, M. Pešic, S. Starschich, T. Schneller, C. Künneth, U. Böttger, H. Mulaosmanovic, T. Schenk, M. H. Park, R. Nigon, P. Muralt, T. Mikolajick, and U. Schroeder, Adv. Electron. Mater. **3**, 1600505 (2017).
[17]M. H. Park, H. J. Kim, Y. J. Kim, Y. H. Lee, T. Moon, K. D. Kim, S. D. Hyun, and C. S. Hwang, Appl. Phys. Lett. **107**, 192907 (2015).
[18]E. D. Grimley, T. Schenk, X. Sang, M. Pešić, U. Schroeder, T. Mikolajick, and J. M. LeBeau, Adv. Electron. Mater. **2**, 1600173 (2016).
[19]H. Mulaosmanovic, J. Ocker, S. Müller, U. Schroeder, J. Müller, P. Polakowski, S. Flachowsky, R. van Bentum, T. Mikolajick, and S. Slesazeck, ACS Appl. Mater. Interfaces **9**, 3792 (2017).
[20]A. K. Tagantsev, I. Stolichnov, N. Setter, J. S. Cross, and M. Tsukada, Phys. Rev. B **66**, 214109 (2002).
[21]U. Schroeder, C. Richter, M. H. Park, T. Schenk, M. Pešić, M. Hoffmann, F. Fengler, D. Pohl, B. Rellinghaus, C. Zhou, C.-C. Chung, J. Jones, and T. Mikolajick, Inorg. Chem. **57**(5), 2752 (2018).
[22]S. V. Kalinin and D. A. Bonnell, Phys. Rev. B **65**, 125408 (2002).
[23]U. Schroeder, W. Weinreich, E. Erben, J. Mueller, L. Wilde, J. Heitmann, R. Agaiby, D. Zhou, G. Jegert, and A. Kersch, ECS Trans. **25**(4), 357 (2009).
[24]W. Weinreich, R. Reiche, M. Lemberger, G. Jegert, J. Müller, L. Wilde, S. Teichert, J. Heitmann, E. Erben, L. Oberbeck, U. Schröder, A. J. Bauer, and H. Ryssel, Microelectron. Eng. **86**, 1826 (2009).
[25]W. Weinreich, T. Tauchnitz, P. Polakowski, M. Drescher, S. Riedel, J. Sundqvist, K. Seidel, M. Shirazi, S. D. Elliott, S. Ohsiek, E. Erben, and B. Trui, J. Vac. Sci. Technol., A **31**, 01A123 (2013).
[26]P. Bintachitt, S. Trolier-McKinstry, K. Seal, S. Jesse, and S. V. Kalinin, Appl. Phys. Lett. **94**, 042906 (2009).
[27]A. Gruverman, D. Wu, and J. F. Scott, Phys. Rev. Lett. **100**, 097601 (2008).
[28]A. Grigoriev, D.-H. Do, D. M. Kim, C.-B. Eom, B. Adams, E. M. Dufresne, and P. G. Evans, Phys. Rev. Lett. **96**, 187601 (2006).
[29]Y. Guan, D. Zhou, J. Xu, X. Liu, F. Cao, X. Dong, J. Müller, T. Schenk, and U. Schroeder, Phys. Status Solidi RRL **9**, 589 (2015).
[30]A. N. Kolmogorov, Izv. Akad. Nauk USSR, Ser. Math. **3**, 355 (1937).
[31]M. Avrami, J. Chem. Phys. **7**, 1103 (1939).
[32]Y. Ishibashi and Y. Takagi, J. Phys. Soc. Jpn. **31**, 506 (1971).
[33]J. Y. Jo, H. S. Han, J.-G. Yoon, T. K. Song, S. H. Kim, and T. W. Noh, Phys. Rev. Lett. **99**, 267602 (2007).
[34]S. Mueller, S. R. Summerfelt, J. Müller, U. Schroeder, and T. Mikolajick, IEEE Electron Device Lett. **33**, 1300 (2012).